

## Erratum: Simplified model for the energy levels of quantum rings in single layer and bilayer graphene [Phys. Rev. B **81**, 045431 (2010)]

M. Zarenia, J. Milton Pereira, A. Chaves, F. M. Peeters, and G. A. Farias  
(Received 16 July 2010; published 29 September 2010)

DOI: [10.1103/PhysRevB.82.119906](https://doi.org/10.1103/PhysRevB.82.119906)

PACS number(s): 71.10.Pm, 73.21.-b, 81.05.U-, 99.10.Cd

The freezing of the radial motion was included in the calculations by means of the substitution  $\frac{\partial}{\partial \rho} \rightarrow 0$  in the Hamiltonians (1) and (16) for single layer and bilayer graphene, respectively, which resulted in the non-Hermitian Hamiltonians (4) and (18). Solving these non-Hermitian Hamiltonians resulted in unphysical non-real values for the energy levels around  $E=0$ . Similar erroneous substitutions were made in e.g. Ref. 1. It was shown in Ref. 2 that the radial part of the angular momentum must be taken zero  $\mathbf{p}_\rho = -i\hbar(\frac{\partial}{\partial \rho} + \frac{1}{2\rho})=0$  in order to guarantee Hermitian Hamiltonians. Because  $\rho=R$  is fixed for a 1D ring we should have substituted  $\frac{\partial}{\partial \rho} \rightarrow -1/2R$  which leads now to Hermitian Hamiltonians and real eigenvalues. Any comments in the paper on imaginary energy are erroneous. Due to this small change many of the formulae and figures have to be modified.

On the left side of Eqs. (4), replace both  $(m+1+\beta)$  and  $(m+\beta)$  by  $(m+\beta+1/2)$  and then Eq. (5) becomes  $\epsilon = \pm \sqrt{(m+\beta+1)(m+\beta)+\delta^2+1/4}$ . Eqs. (6) and (7) should be removed. Now the energy values are real and therefore the discussion below Eq. (7) starting from the second sentence should be removed. In Eqs. (11) and (13) replace  $\beta$  by  $\beta+1/2$  and replace Eq. (14) by

$$\frac{j}{v_F} = \left( \frac{\partial \epsilon}{\partial \beta} \right)_K + \left( \frac{\partial \epsilon}{\partial \beta} \right)_{K'} + (\epsilon^2 + \delta^2) \left[ \frac{2(m+\beta+1)}{\epsilon(\epsilon^2 - \delta^2)} \right].$$

Replace the sentence below Eq. (14) by: “Since for the ground state energy  $m+\beta=-1/2$  where  $\partial\epsilon/\partial\beta=0$  the last term in Eq. (14) is zero and the total current oscillates around zero.”

In the first paragraph in Sec. II B replace the following formula  $E = \pm \sqrt{m(m+1)(\hbar v_F/R)^2 + \Delta^2}$  by

$$E = \pm \sqrt{[(m+1/2)(\hbar v_F/R)]^2 + \Delta^2}.$$

Also remove the following part from this paragraph: “Note that for  $m=0$  and  $m=-1$  the energy  $E = \pm \Delta$  is independent of  $R$  and all branches are two-fold degenerate” and the discussion at the end of this paragraph should be corrected as: “For small radii,  $E \approx \pm \hbar v_F |m+1/2|/R$  and all branches diverge as  $1/R$ .”

In the third paragraph in Sec. II B replace  $\epsilon^2 - [(m+\Phi/\Phi_0)+1/2]^2 = \delta^2 - 1/4$  by  $\epsilon^2 - [(m+\Phi/\Phi_0)+1/2]^2 = \delta^2$ ;  $\delta = \Delta/E_0 = 1/2$  by  $\delta = \Delta/E_0 = 0$  and  $\delta > 1/2$  by  $\delta > 0$ . Remove Fig. 4 and the last sentences at the end of this paragraph should be corrected as “The energy in this case is  $\epsilon = \pm \sqrt{\beta(\beta+1)+\delta^2+1/4}$  which for  $\delta=0$  becomes  $\epsilon = \pm |\beta+1/2|$ .”

In the fourth paragraph the formula  $\Delta\epsilon = 2\sqrt{\delta^2-1/4}$  should be replaced by  $\Delta\epsilon = 2\delta$ . The following part also

should be removed from the end of paragraph: “Notice also that the  $m=-2$  level only exists for  $\Delta \geq E_0/2$ , i.e. for  $\Delta < E_0/2$  there is no real energy solution when  $m=-2$ .”

In the last paragraph in Sec. II B the explanation about Fig. 8 should be corrected by “Note that the contribution from the  $K$ -valley  $j_K$  [Fig. 8(a)] and the  $K'$ -valley  $j_{K'}$  [Fig. 8(b)] are the same and they oscillate in phase around zero.” Replace Eq. (18) by

$$-(\epsilon - \tau u_1) \phi_A(R) - \left( m + \beta - \frac{1}{2} \right) \phi_B(R) + t' \phi_C(R) = 0,$$

$$\left( m + \beta - \frac{1}{2} \right) \phi_A(R) + (\epsilon - \tau u_1) \phi_B(R) = 0,$$

$$t' \phi_A(R) - (\epsilon - \tau u_2) \phi_C(R) + \left( m + \beta + \frac{1}{2} \right) \phi_D(R) = 0,$$

$$\left( m + \beta + \frac{1}{2} \right) \phi_C(R) - (\epsilon - \tau u_2) \phi_D(R) = 0,$$

and Eq. (19) by

$$\begin{aligned} & (\epsilon - \tau u_1)^2 \left[ (\epsilon - \tau u_2)^2 - \left( m + \beta + \frac{1}{2} \right)^2 \right] - \left( m + \beta - \frac{1}{2} \right)^2 \\ & \times \left[ (\epsilon - \tau u_2)^2 - \left( m + \beta + \frac{1}{2} \right)^2 \right] - (\epsilon - \tau u_1)(\epsilon - \tau u_2)t'^2 \\ & = 0, \end{aligned}$$

and Eq. (20) by

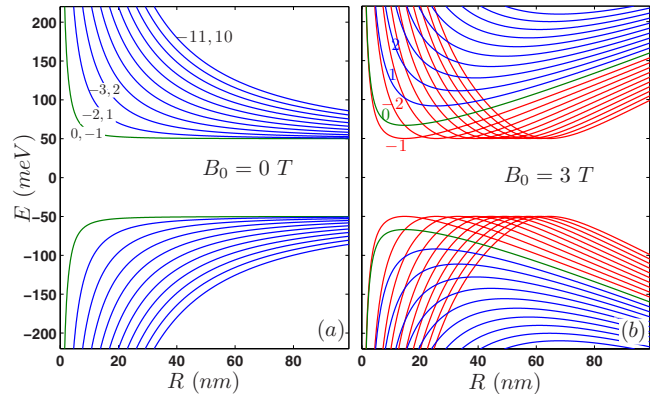


FIG. 1. (Color online) Energy levels with  $m=-10, \dots, 10$  of single layer graphene quantum ring as function of ring radius  $R$  for  $B_0=0$  T (left panel) and  $B_0=3$  T (right panel) when the mass term is  $\Delta=50$  meV.

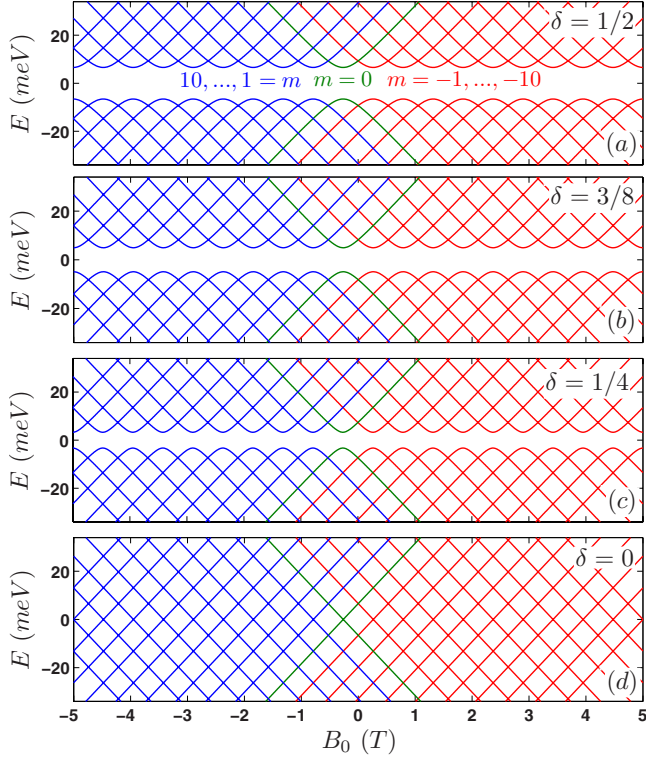


FIG. 3. (Color online) Electron and hole energy levels of a single layer graphene quantum ring as function of external magnetic field  $B_0$  for (a)  $\delta=1/2$ , (b)  $\delta=3/8$ , (c)  $\delta=1/4$ , and (d)  $\delta=0$  with  $R=50$  nm, and total angular quantum number  $-10 \leq m \leq -1$  (red curves),  $1 \leq m \leq 10$  (blue curves), and  $m=0$  (green curves).

$$s^4 - 2s^2[(m + \beta)^2 + \delta^2 + (t')^2/2 + 1/4] + 4s\tau\delta(m + \beta) + [(m + \beta)^2 - 1/4]^2 - 2\delta^2[(m + \beta)^2 - (t')^2/2 + 1/4] + \delta^4 = 0,$$

and Eq. (21) by

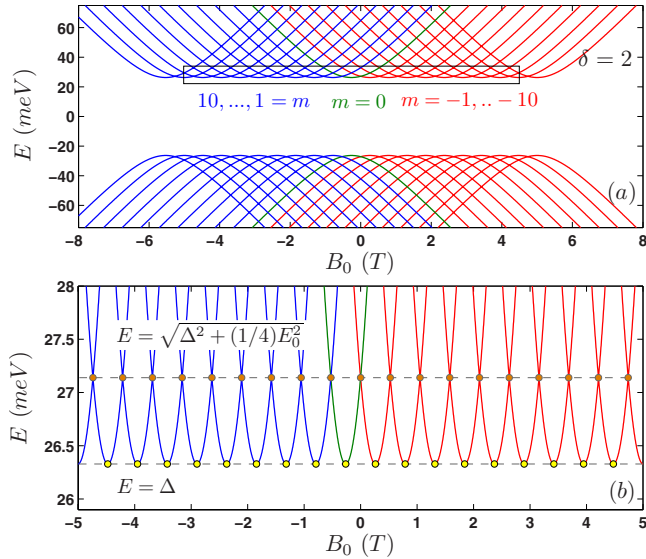


FIG. 5. (Color online) (a) Electron and hole energy levels of a single layer graphene quantum ring as function of external magnetic field  $B_0$  for  $\delta=2$  and  $R=50$  nm. (b) An enlargement of the region which is shown in (a) by a rectangle.

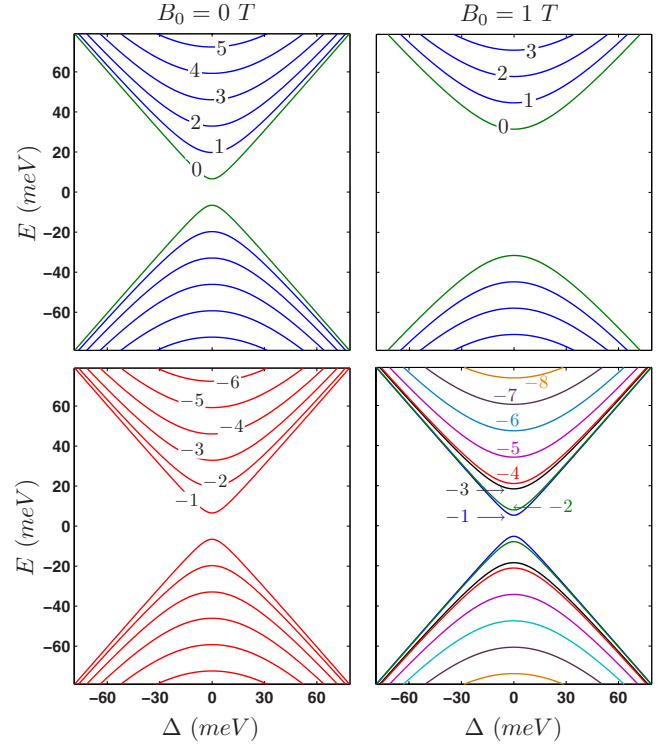


FIG. 6. (Color online) Lowest energy levels of a single layer graphene quantum ring as function of the mass term  $\Delta$  with  $B_0 = 0$  T (left panels) and  $B_0=1$  T (right panels) for  $m \geq 0$  (upper panels) and  $m < 0$  (lower panels) with  $R=50$  nm.

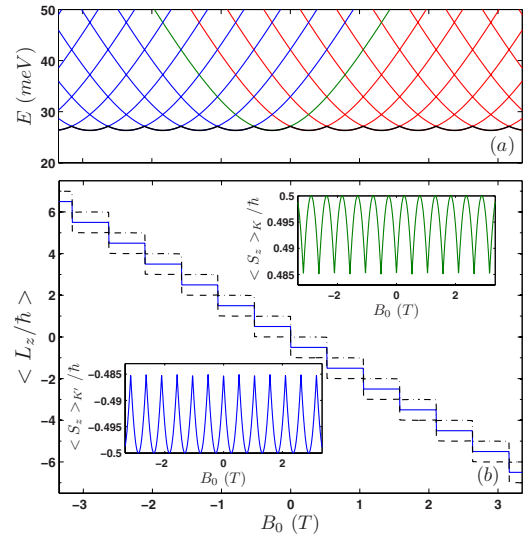


FIG. 7. (Color online) (a) Electron energy levels of a graphene single layer quantum ring as function of external magnetic field  $B_0$  for the same parameters as used in Fig. 5. Black curve shows the ground-state energy. (b) Ground-state expectation value of  $L_z/\hbar$  as function of magnetic field for both  $K$  (black dashed curve) and  $K'$  valleys (black dash-dotted curve). Expectation value of  $S_z/\hbar$  versus magnetic field is plotted in the upper inset for  $K$  valley and in the lower inset for  $K'$  valley. The blue solid curve shows the expectation value  $\langle J_z \rangle$  which is the same for both valleys.

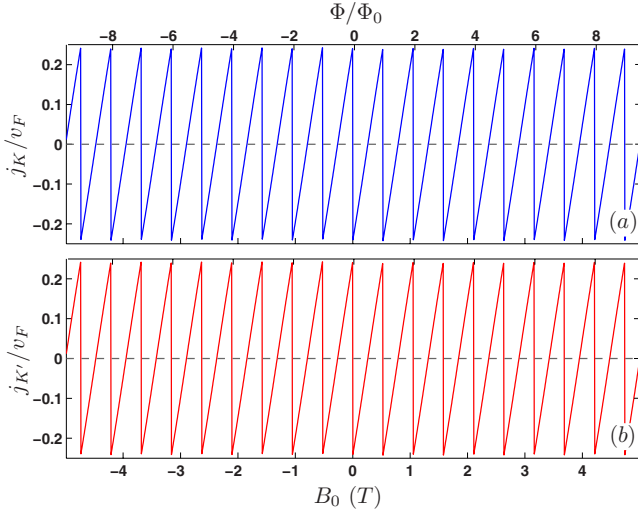


FIG. 8. (Color online) The angular current density in the (a)  $K$  valley and (b)  $K'$  valley of a monolayer graphene quantum ring as function of external magnetic field  $B_0$  for the ground-state energy shown by the black curve in Fig. 7(a).

$$s_{\pm}^2 = (m + \beta)^2 + (t')^2/2 + 1/4 \pm \sqrt{(t')^4/4 + (m + \beta)^2[(t')^2 + 1/2] + (t')^2/4}.$$

After Eq. (21) the following part should be removed: “These are real when  $|m + \beta| \geq 1$ . In the opposite case of  $|m + \beta| < 1$  (or equivalently  $-1 + \beta < m < 1 - \beta$ ) we have  $s_{\pm}^2 < 0$  and

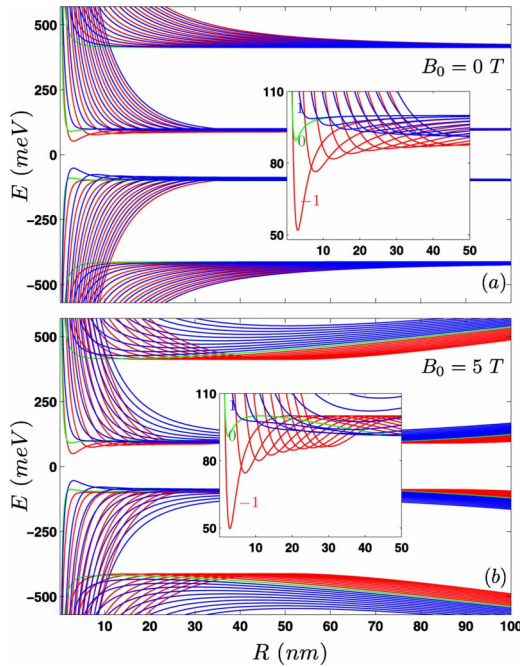


FIG. 9. (Color online) Lowest energy levels of a bilayer graphene quantum ring as function of ring radius  $R$  with (a)  $B_0 = 0$  T and (b)  $B_0 = 5$  T for  $U_b = 100$  meV and total angular quantum number  $-10 \leq m \leq -1$  (red curves),  $1 \leq m \leq 10$  (blue curves), and  $m = 0$  (green curves). The insets are an enlargement of the small energy and small  $R$  region.

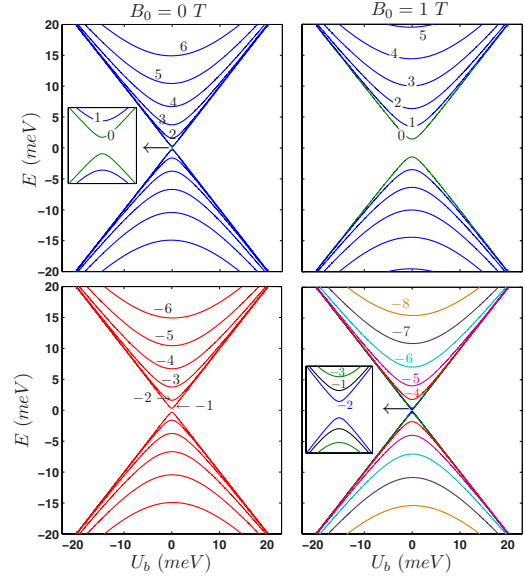


FIG. 13. (Color online) Lowest energy levels of a bilayer graphene quantum ring as function of the gate potential  $U_b$  when  $B_0 = 0$  T (left panels) and  $B_0 = 1$  T (right panels) for  $m \geq 0$  (upper panels) and  $m < 0$  (lower panels) with  $R = 50$  nm.

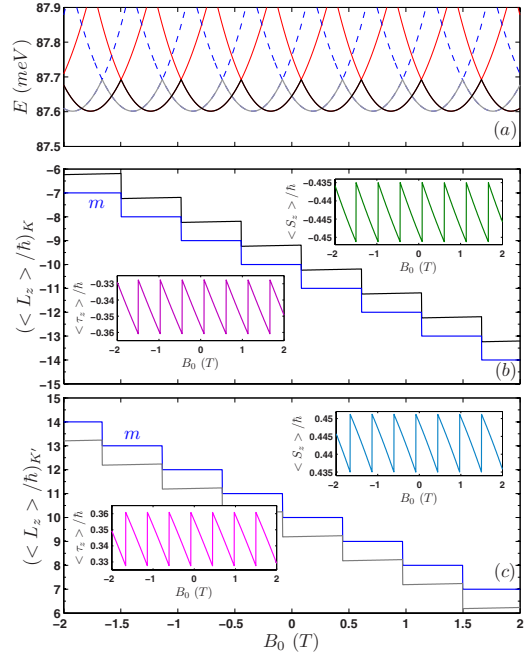


FIG. 14. (Color online) (a) Electron energy levels of a bilayer graphene quantum ring as function of external magnetic field  $B_0$  for a quantum ring of radius  $R = 50$  nm and with  $U_b = 100$  meV for both the  $K$  valley (solid curves) and the  $K'$  valley (dashed curves). Black curve shows the ground-state energy of the energy spectrum in the  $K$  valley whereas the gray curve the corresponding ground-state energy of the  $K'$  valley. (b) Ground-state expectation values of  $L_z/\hbar$ ,  $S_z/\hbar$ , and  $\tau_z/\hbar$  as function of magnetic field in the  $K$  valley. The blue solid curve shows the expectation value of  $J_z/\hbar$  operator. (c) The same as (b) but for the  $K'$  valley.

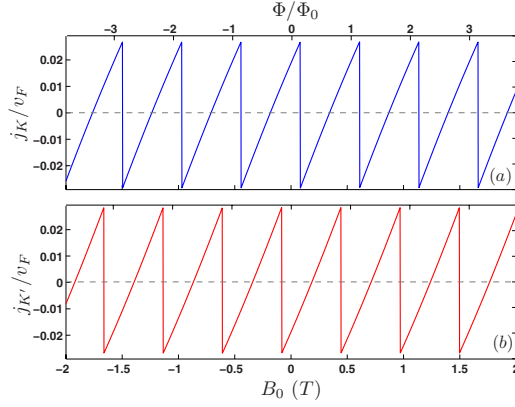


FIG. 15. (Color online) The ground-state angular current density in the (a)  $K$  valley and (b)  $K'$  valley of a bilayer graphene quantum ring as function of external magnetic field  $B_0$  with  $U_b=100$  meV and  $R=50$  nm.

consequently the corresponding energies are imaginary.” Replace the formula  $s^2=(m+\beta)^2[(m+\beta)^2-1]/(t')^2$  by  $s^2=[(m+\beta)^2-1/4]^2/[(t')^2+1/2]$  and also replace Eq. (22) by

$$s \approx \pm [(m+\beta)^2-1/4]/\sqrt{(t')^2+1/2}.$$

Replace Eq. (28) by

$$\phi_A(R) = 1, \quad \phi_B(R) = -\frac{m+\beta-1/2}{\epsilon-\tau u_1},$$

$$\phi_C(R) = \frac{(\epsilon-\tau u_1)^2-(m+\beta-1/2)^2}{t'(\epsilon-\tau u_1)},$$

$$\phi_D(R) = \frac{(m+\beta+1/2)[(\epsilon-\tau u_1)^2-(m+\beta-1/2)^2]}{t'(\epsilon-\tau u_1)(\epsilon-\tau u_2)}$$

and Eq. (30) should be corrected as

$$j = \sum_{\tau=\pm 1} \frac{2v_F}{\epsilon-\tau u_1} \times \left[ (m+\beta-1/2) + \frac{(m+\beta+1/2)[(\epsilon-\tau u_1)^2-(m+\beta-1/2)^2]}{t'^2(\epsilon-\tau u_1)(\epsilon-\tau u_2)} \right].$$

In the first paragraph in Sec. III B the explanation for Fig. 9 should be corrected as follows: “As compared to the single layer quantum ring results of Fig. 1, we find that we have a second set of levels that for large  $R$  are displaced in energy by  $t$ .” Replace the formula  $(m+\beta)^2[(m+\beta)^2-1]$  by  $[(m+\beta)^2-1/4]^2$  and remove these sentences: “For  $m=-1, 0, 1$  the behavior of the spectrum is different and the corresponding energy levels do not diverge when  $R \rightarrow 0$ . The same behavior was found for the single layer results, but only for  $m=0, -1$ .”

In the second paragraph of Sec. III B replace  $E(0)=E(1)=E(-1)$  by  $E(0) \approx E(1) \approx E(-1)$  and remove the following part: “Notice that here we found that for  $m=-1$  and  $m=-2$  no real energy solution is found for  $U_b$  below some critical value.”

In Sec. IV replace the relation  $\Delta > \hbar v_F/2R$  by  $\Delta > 0$ .

Now by solving the Hermitian Hamiltonian for single layer graphene quantum rings all the values of the energy levels are uniformly shifted by  $|\Delta - \sqrt{\Delta^2 - (1/4)E_0^2}|$ . Therefore for the parameters in Fig. 2 the values of the energy levels are shifted by 0.43 meV while in Fig. 5 the energy levels are shifted by 0.8359 meV. In Fig. 5(b) replace  $E = \sqrt{\Delta^2 - (1/4)E_0^2}$  by  $E = \Delta$  (yellow points) and replace  $E = \Delta$  by  $E = \sqrt{\Delta^2 + (1/4)E_0^2}$  (orange points).

The shift in the energy levels of the bilayer graphene quantum rings is too small (i.e. of order 0.1 meV) and thus, Figs. 10, 11, and 12 remain unchanged.

Figures 8(c) and 15(c) are unchanged and are not repeated here.

The authors are grateful to B. Trauzettel for pointing out the non-Hermiticity of the Hamiltonian.

<sup>1</sup>A. G. Aronov and Y. B. Lyanda-Geller, *Phys. Rev. Lett.* **70**, 343 (1993).

<sup>2</sup>F. E. Meijer, A. F. Morpurgo, and T. M. Klapwijk, *Phys. Rev. B* **66**, 033107 (2002).